

# Evolution of the crystal-field splittings in the compounds CeX (X=P, As, Sb, Bi), CeY (Y=S, Se, Te) and their alloys CeX<sub>1-x</sub>Y<sub>x</sub>

P. Roura-Bas <sup>a</sup>, V. Vildosola <sup>a</sup> and A. M. Llois <sup>a,b</sup>

<sup>a</sup> Dpto de Física, Centro Atómico Constituyentes, Comisión Nacional de Energía Atómica and

<sup>b</sup> Dpto de Física, Universidad de Buenos Aires, Buenos Aires, Argentina

The crystal-field splittings of the monpnictides and monochalcogenides of Cerium (CeX and CeY) and their alloys (CeX<sub>1-x</sub>Y<sub>x</sub>) are calculated by means of an *ab initio* many-body combined technique. The hybridization functions of the 4f states of Cerium with the conduction band for each material are obtained from first principles within the local density approximation (LDA) and are used as input for the Anderson impurity model, which is solved within a multi-orbital Non-Crossing Approximation (NCA). This realistic theoretical approach (LDA-NCA) is able to reproduce the experimental results for the crystal-field splittings of the CeX and CeY series in agreement with previous theoretical calculations. It is also able to describe the non-linear evolution of the splittings in the CeX<sub>1-x</sub>Y<sub>x</sub> alloys as a function of x. An analysis of the values of the crystal-field splittings in all the compounds can be done in depth in this contribution, due to a detailed knowledge of the band structure and crystal environment in combination with many-body physics.

## I. INTRODUCTION

One of the important issues of the last years has been to produce realistic theoretical descriptions of strongly correlated electronic systems. These descriptions make a point out of including detailed electronic structure information as well as many body dynamical effects on an equal footing. Examples of materials for which this kind of treatments becomes essential are Cerium compounds. In these systems, the Cerium atom is very sensitive to the crystalline and chemical environment and the differences in the interaction strengths of the localized 4f states with the conduction band can give rise to a wide variety of behaviors. A lot of effort has been devoted to implement realistic calculations using different approaches [1, 2, 3].

In this work, we apply a mixed *ab initio* many-body technique to study the monpnictides CeX (X=P, As, Sb, Bi), the monochalcogenides CeY (Y=S, Se, Te) and CeX<sub>1-x</sub>Y<sub>x</sub> alloys which exhibit interesting and unusual physical properties. These compounds crystallize in the simple rock-salt structure making it possible to study in depth the influence of the electronic structure on their properties. In particular, the heavier compounds, namely CeSb, CeBi and CeTe [4] present a strong magnetic anisotropy, great sensitivity to the application of pressure and to the dilution of Cerium by non magnetic ions, as well as to the substitution of a pnictogen by another pnictogen or by a chalcogen[5]. These heavier compounds also show, in particular, anomalous small values for the 4f crystal-field splittings ( $\Delta_{CF}$ ) as compared to the other compounds within the series. We are interested here in doing a thorough analysis of the crystal field splittings as well as of the symmetry of the 4f states in these Ce compounds, for which is necessary to disentangle the interactions among the 4f states and the environment. We focus, thereafter, on the study of the crystal field splitting within the CeX and CeY series and also on its evolution along the CeX<sub>1-x</sub>Y<sub>x</sub> alloys as a function of x.

The anomalous value of the crystal field splitting of

the heavier CeX and CeY compounds has been previously treated and understood by Wills and Cooper [1, 6]. These authors showed that the dominant contribution to the splittings in these monpnictides can be obtained from the point-charge (PC) model which is appropriate for insulators and ionic systems. But the depression of the splitting along the series can only be understood if hybridization effects are taken into account. The PC model accounts well for the splittings of rare earth monpnictides when the rare earth goes from Pr to Tb, but it fails to describe Ce systems because in these compounds the 4f-band hybridization with the conduction states cannot be neglected. Wills and Cooper considered that the total splitting in these systems is the result of two independent contributions: the extrapolated value from the PC model considering non-hybridized 4f levels and the splittings induced by hybridization. They calculated the 4f hybridization function out of the conduction band density of states obtained using the linear muffin-tin-orbital (LMTO) method within the atomic-sphere approximation (ASA) for the self consistent potential. This last approximation does not consider the anisotropy of the crystalline environment. Within these calculations the authors treated the 4f state as belonging to the core. They obtained the hybridization contribution to  $\Delta_{CF}$  on the basis of the Anderson hamiltonian solved to second order in perturbation theory.

In the present work, we obtain the  $\Delta_{CF}$  's in a different way, we perform *ab initio* calculations using the Full Potential-LAPW method within the local density approximation (LDA) [7] and treat the 4f states as part of the valence band. We then compute the 4f hybridization function following ref.[2, 8]. This function contains detailed information on the electronic structure of each system and is used as input for the Anderson impurity hamiltonian which is solved within a multiorbital non-crossing approximation (NCA). This LDA-NCA approach has already been applied to cubic and tetragonal Ce based systems to calculate  $\Delta_{CF}$ 's and to ob-

tain trends in the Kondo energy scales, yielding results which are in good agreement with the available experimental information [2, 9]. We calculate the crystal field splittings for CeX and CeY and compare them with the previous theoretical results and with experimental data. We also follow the evolution of  $\Delta_{CF}$  with concentration for the CeSb<sub>1-x</sub>Te<sub>x</sub> alloys, which had not been previously theoretically approached, and compare the results with experimental data. We also analyse the behavior of CeAs<sub>1-x</sub>Se<sub>x</sub>, which has not been previously tackled either experimentally nor theoretically.

In section 2 we give a brief description of the LDA-NCA technique. Section 3 is divided into three parts: a) results for the  $\Delta_{CF}$  splittings of the CeX monpnictides, b) Comparison of the  $\Delta_{CF}$  splittings of the two series, CeX and CeY, and c) study of the evolution of  $\Delta_{CF}$  for the CeX<sub>1-x</sub>Y<sub>x</sub> alloys. Finally, in section 4 we discuss and conclude.

## II. METHOD OF CALCULATION

The LDA-NCA approach is an *ab initio* many body technique that solves the Anderson impurity problem using as input the hybridization function,  $\Gamma(\epsilon)$ , of the conduction band with the 4f-state of Ce. The hybridization function is calculated from first principles within the Density Functional Theory. In this work, the *ab initio* calculations are done using the full potential linearized augmented plane waves method (FP-LAPW), as implemented in the Wien2k code [10].

For Ce systems the Anderson impurity hamiltonian has the form:

$$H = \sum_{k\sigma} \varepsilon_{k\sigma} c_{k\sigma}^\dagger c_{k\sigma} + \sum_m \varepsilon_{fm} f_m^\dagger f_m + U \sum_{m>m'} n_{fm} n_{fm'} + \sum_{k\sigma, m} (V_{k\sigma, m} f_m^\dagger c_{k\sigma} + H.C.), \quad (1)$$

where  $V_{k\sigma, m}$  is the hopping matrix element between the conduction electron states, ( $c_{k\sigma}$ ), and the 4f orbitals ( $f_m$ ),  $\varepsilon_{fm}$  is the corresponding 4f-energy level with respect to the Fermi energy and  $U$  the on-site Coulomb repulsion of the 4f electrons.  $\Gamma(\varepsilon)$  is proportional to the product  $V_{k\sigma, m}^* V_{k\sigma, m'}$  and, as suggested by *Gunnarsson et al.* [8], it can be estimated from the projected LDA 4f density matrix  $\rho_{mm'}^{LDA}$  at the Ce site in the following way,

$$\Gamma_{mm'}(\varepsilon) = -Im \left\{ \lim_{\eta \rightarrow 0} \left[ \left( \int dz \frac{\rho_{mm'}^{LDA}(z)}{\varepsilon - i\eta - z} \right) \right]^{-1} \right\}. \quad (2)$$

In all cases the labels  $m$  and  $m'$  correspond to the different irreducible representations of the 4f states at the cubic Ce site. That is, for  $J = \frac{5}{2}$  the doublet  $\Gamma_7$  and the quartet  $\Gamma_8$ , while for  $J = \frac{7}{2}$  the doublets  $\Gamma_6$  and  $\Gamma_7$  and the quartet  $\Gamma_8$ .

The  $U \rightarrow \infty$  limit of the Anderson impurity model is solved by using the slave boson technique within the non crossing approximation (NCA). The NCA equations consist of a couple of integral nonlinear equations for the pseudo-boson ( $f^0$ ) and pseudo-fermion ( $f^1$ ) self-energies, each of them containing the hybridization function  $\Gamma_{mm'}(\varepsilon)$ . This  $U \rightarrow \infty$  limit is reasonable to obtain crystal field splittings, because the splittings are stable within a wide temperature range above the Kondo temperature. For a detailed review of the NCA formalism see Ref [11, 12].

With the LDA-NCA technique one can calculate the crystal-field splittings and also obtain the symmetry of the ground state and excited 4f levels. The crystal-field splittings are read from the separation of the peaks of the different spectral functions,  $\rho_{mm}$ 's, which are shifted one with respect to the other due to the different degree of hybridization of each 4f level with the conduction band. We focus on the value of the splitting corresponding to the  $J = \frac{5}{2}$  multiplet, namely  $\Delta_{CF} = \varepsilon_{f\Gamma_7} - \varepsilon_{f\Gamma_8}$ .

## III. RESULTS

The LDA calculations are performed at the experimental volumes for the CeX and CeY compounds. The *muffin-tin* radii,  $R_{mt}$  are taken equal to 2.4 a.u. in the case of Ce, while the corresponding radii for the anion ligand varies from 1.6 a.u. to 2.8 a.u. depending on the atomic radius. 102 **k** points in the irreducible Brillouin zone are considered to be enough for the quantities to be calculated.

In the NCA-equations the 4f state has a bare energy value, which we take from photoemission experiments. It is namely, -3 eV for the series CeX, -2.6 eV for CeTe and -2.4 eV for, both, CeS and CeSe. All these energy levels are given with respect to the Fermi energy [13].

Within NCA the self energies and the Green's functions are self-consistently obtained by considering the spectrum up to 6500 K above the Fermi level for the more delocalized systems (Y=S, Se, X=P, As) and up to 5000 K for the more localized ones (Y=Te, X=Sb).

### A. Crystal-field splittings in CeX

We discuss in this section the main features of the hybridization functions along the CeX series in order to understand the evolution of the crystal-field splittings. As a representative example, we show in Figure 1 the calculated hybridization functions for the  $\Gamma_7$  and  $\Gamma_8$  symmetries corresponding to CeAs. In the inset, the detailed structure within an energy window around the Fermi level is given.

It can be observed that the hybridization functions are very rich in structure. Far below and far above the Fermi level the  $\Gamma_8$  symmetry is the one with the largest hybridization contribution, while close to the Fermi level

the  $\Gamma_7$  one is stronger. This feature, with varying relative weights, holds on for all the systems under study. The different relative weights are the finger prints which determine the evolution of the crystal-field splittings. As it will be shown in the next section, the  $4f$  states with  $\Gamma_7$  symmetry hybridize mainly with the  $5d$ -Ce band while the ones with  $\Gamma_8$  symmetry do it mainly with the anion  $p$  states.

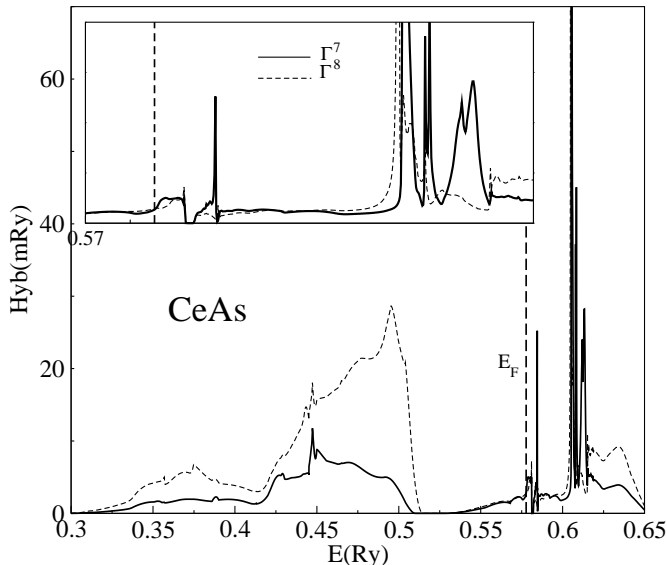


Figure 1: Hybridization function of the  $4f$  states with the conduction band for CeAs :  $\Gamma_7$  (solid curve) and  $\Gamma_8$  (dashed curve) symmetries. In the inset, a zoom of an energy range around the Fermi level is given.

Due to the ionic character of the Ce compounds under study, the LDA unoccupied part of the spectrum is particularly ill given. Taking this into account, in order to reproduce the trends of the  $\Delta_{CF}$ 's, we consider in this work the energy spectrum up to an energy of the order of 6000 K above the Fermi level. Together with the correct trends in the splittings, we also obtain the experimental ground state symmetry, namely the  $\Gamma_7$ , for all these systems. These results show that for these compounds the energy spectrum around the Fermi energy determines the symmetry of the ground state, even if the  $\Gamma_8$  hybridization function is the strongest one in the average.

The calculated values for the splittings are: 165 K for CeP, 155 K for CeAs, 70 K for CeSb and 50 K for CeBi. The obtained values and trends are in agreement with experiments and with the previous theoretical work. The calculations reproduce properly the sharp decrease of the splittings when going from CeAs to CeSb.

In order to understand the depression of  $\Delta_{CF}$  in CeSb and CeBi as compared to CeP and CeAs[14], we perform a calculation for CeP but at the experimental volume of CeBi, which is the largest one in the series. The effect of the negative pressure is, as expected, a reduction in the strength of the hybridization functions due to larger interatomic distances. Around the Fermi level this

reduction is more pronounced for the  $\Gamma_7$  than for the  $\Gamma_8$  symmetry. This decrease in the hybridization difference between both symmetries gives rise to a decrease in the value of the splitting. That is, the observed jump in the splittings along the series is correlated with a jump in volume when going from CeAs to CeSb. This analysis also applies to the CeY series (Ce monochalcogenides).

## B. Crystal field splittings in CeY vs CeX

Due to the extra  $p$ -electron of the Y-anion, the  $\Gamma_8$  symmetry is more strongly hybridized in the CeY series than along the CeX one. The  $\Gamma_7$  hybridization is of the same order of magnitude in both series, as it can be drawn from the comparison of Fig. 2 and Fig. 3. In these figures CeS and CeP are shown as examples. The same behavior applies for the other compounds.

In the inset of figures 2 and 3 the partial  $p$ - and  $5d$ -densities of states are plotted in detail. Comparing these densities of states with the corresponding hybridizations, it can be observed that below  $E_F$ ,  $\Gamma_8$  hybridizes essentially with the  $p$ -states of the X and Y anions, while  $\Gamma_7$  does it with the  $5d$ -states of the neighbouring Ce atoms.

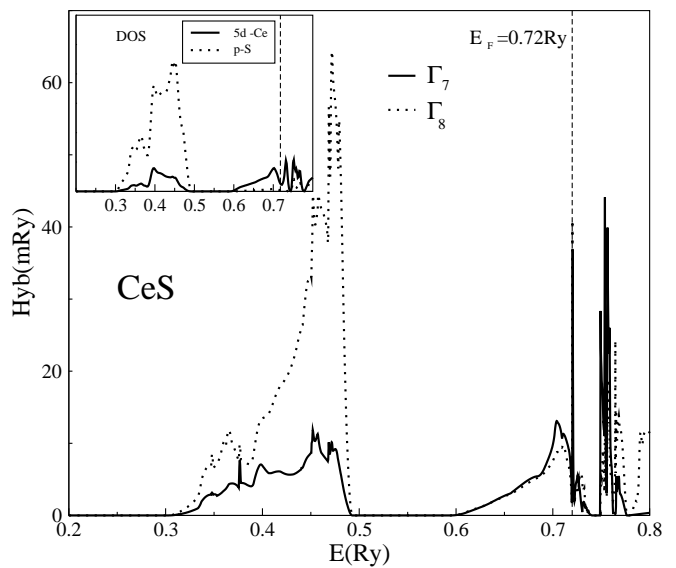


Figure 2: Calculated hybridization functions for CeS:  $\Gamma_7$  symmetry (solid curve) and  $\Gamma_8$  symmetry (dotted curve). Inset:  $5d$ -DOS for Ce (solid curve) and  $p$ -DOS for the anion S (dotted curve).

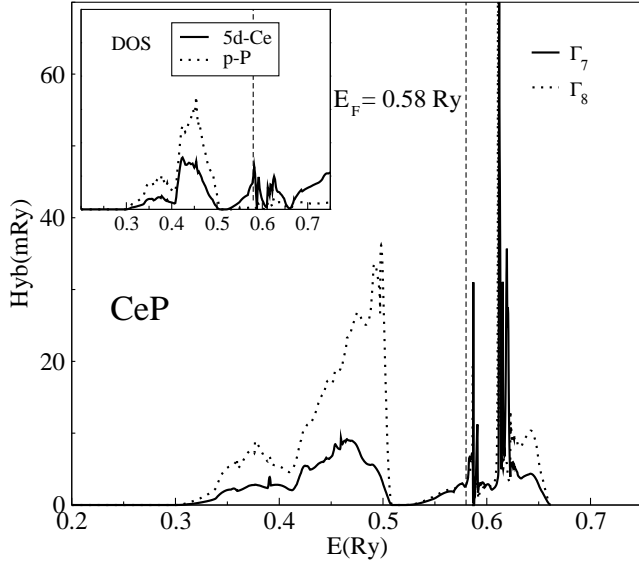


Figure 3: Calculated hybridization functions for CeP:  $\Gamma_7$  symmetry (solid curve) and  $\Gamma_8$  symmetry (dotted curve). Inset:  $5d$ -DOS for Ce (solid curve) and  $p$ -DOS for the anion P (dotted curve).

Y	$\Delta_{CF}^{exp}$	$\Delta_{CF}^{NCA}$	X	$\Delta_{CF}^{exp}$	$\Delta_{CF}^{NCA}$
S	140	150	P	172	165
Se	116	120	As	159	155
Te	32	50	Sb	37	70

Table I: Experimental and LDA-NCA results for the crystal-field splittings,  $\Delta_{CF} = E(\Gamma_8) - E(\Gamma_7)$ , in the CeX and CeY series. The splittings are given in Kelvin. See Ref [14, 15] for the experimental data.

The values of the calculated  $\Delta_{CF}$ 's, shown in Table I are in very good agreement with the experimental results. The order of magnitude as well as the evolution of the  $\Delta_{CF}$ 's are similar in both series. It should be noticed that the values corresponding to the CeY compounds are slightly smaller than the ones of the CeX series, and this is well reproduced in the calculations.

In spite of the larger values of the  $\Gamma_8$  hybridization function for energies lying far below the Fermi level, the splittings are determined mainly by the hybridization character near the Fermi energy. The extra electron of the CeY compounds, as compared to the CeX ones, does not change the symmetry of the ground state nor that of the excited ones, preserving the order of magnitude of the  $\Delta_{CF}$ 's when going from CeX and CeY.

The feature which differentiates the two series under study, namely, the slightly smaller splitting observed in the CeY series as compared to the CeX one, can be correlated to the behavior of the partial  $5d$  densities of states at the Fermi level. As it can be observed in the *inset* of Fig. 2 and 3, the Fermi level falls in a maximum of the  $5d$ -DOS for CeP and in a valley of the  $5d$ -DOS in the case of CeS. The  $p$ -DOS, on the other hand, does not

change considerably when going from CeP to CeS. The larger value of the  $5d$ -DOS near  $E_F$  implies a larger  $\Gamma_7$  hybridization, which in turn gives rise to a larger splitting for CeP than for CeS. This behavior of the partial  $5d$ -DOS at the Fermi level also holds for the other compounds.

### C. From CeX to CeY: Crystal-field splittings in the $\text{CeX}_{1-x}\text{Y}_x$ alloys

So far, until now we have made a comparative analysis of the evolution of the  $\Delta_{CF}$ 's along the two series CeX and CeY, the difference between them being the extra  $p$ -electron of the Y atoms as compared to the X ones. The  $\Delta_{CF}$ 's of the solid solutions  $\text{CeSb}_{1-x}\text{Te}_x$  were measured by inelastic neutron scattering by *Rossat* [16] for different *Te*-concentrations ( $x = 0.05, 0.1, 0.5$  and  $0.7$ ). The experimental data are shown in the upper plot of Figure 4. To the best of our knowledge, there is no previous theoretical work interpreting the shown results and complementing the suggestions done by *Rossat* in the sense that the observed trends in the alloys should be associated to  $p-f$  mixing.

In order to understand the non linear evolution of  $\Delta_{CF}$  as a function of *Te* concentration, we simulate the substitution of *Sb* by *Te*, and viceversa, by doing electronic structure calculations within the virtual-crystal approximation[17, 18] (VCA) in the two concentration limits. We have also analysed the splittings of the lighter  $\text{CeAs}_{1-x}\text{Se}_x$  alloys within the same approximation. To this purpose, we add a small amount of valence electrons to the X atom of CeX and withdraw small amounts of valence electrons from the Y atom of CeY. Charge neutrality is preserved in the calculations. Nearly one third of the added charge goes to the  $p$  levels of the anions, while the rest goes to the interstitial region. The occupation of the  $5d$  and  $4f$  levels of the Ce atoms, remains unchanged. Within this approach the original crystal symmetry is preserved.

In the case of  $\text{CeSb}_{1-x}\text{Te}_x$ , we calculate the values of the splittings for four different VCA concentrations, namely by adding 0.1- and 0.2-electrons to *Sb* and by subtracting 0.1- and 0.2-electrons from *Te* in the parent compounds *CeSb* and *CeTe*, respectively. In order to compare with the behavior in the lighter alloys  $\text{CeAs}_{1-x}\text{Se}_x$ , we consider for these last systems two concentrations, one adding 0.2e to *As* and the other subtracting this same amount of electrons from *Se*. In all cases the VCA calculations are done at the experimental volume of the corresponding parent compounds, as we are just studying here the electronic contribution to the evolution of the  $\Delta_{CF}$  values. In the first case, the obtained splittings are  $\Delta_{CF}(\text{CeSb} + 0.1e) = 90$  K,  $\Delta_{CF}(\text{CeSb} + 0.2e) = 120$  K,  $\Delta_{CF}(\text{CeTe} - 0.1e) = 55$  K and  $\Delta_{CF}(\text{CeTe} - 0.2e) = 100$  K. For the second simulated alloys the values are  $\Delta_{CF}(\text{CeAs} + 0.2e) = 200$  K and  $\Delta_{CF}(\text{CeSe} - 0.2e) = 200$  K. According to the exper-

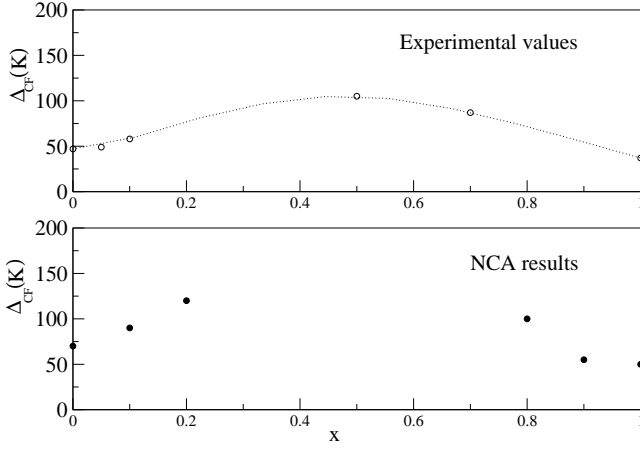


Figure 4: Calculated  $\Delta_{CF}$ 's of  $\text{CeSb}_{1-x}\text{Te}_x$  systems. We have denoted  $\text{CeSb}+0.1$  and  $\text{CeSb}+0.2$  as  $x = 0.1$  and  $x = 0.2$  and  $\text{CeTe}-0.2$  and  $\text{CeTe}-0.1$  as  $x = 0.8$  and  $x = 0.9$ , respectively. Experimental and calculated results are given in Kelvin. See Ref. [16] for experimental data.

imental trends for  $\text{CeSb}_{1-x}\text{Te}_x$ , we obtain an increase in the value of the crystal-field splittings when a small amount of charge is added to  $\text{CeSb}$  and also when it is taken away from  $\text{CeTe}$ , as it is shown in Figure 4. For the lighter alloys there is no available experimental results for the splittings, but we obtain the same behavior as for the other ones.

When  $\text{CeX}$  is doped with a small amount of charge the value of the  $\Gamma_8$  hybridization function increases slightly for energies below  $E_F$ . This is due to an increasing  $4f$ - $p$  mixing in that energy region. This extra charge also affects indirectly the  $4f$ - $5d$  hybridization through an increased  $p$ - $5d$  mixing. This indirect mechanism induces a slight increment of the  $\Gamma_7$  hybridization function around  $E_F$ . There is no considerable contribution to the crystal-field splittings from energies lying more than 0.03 Ryd below  $E_F$ , because the hybridization functions of both symmetries change by a similar amount. This can be seen in Figure 5. However, above  $E_F$ , the  $\Gamma_8$  hybridization goes down due to a decreasing number of unoccupied  $p$  states, while the  $\Gamma_7$  hybridization function goes up, these two effects give rise to an increase in the value of  $\Delta_{CF}$ . These results agree with the experimental ones obtained by Rossat *et al.* and the output of our calculations reinforce the interpretation done by them.

In the other concentration limit, when a small amount of charge is removed from  $\text{Te}$  in  $\text{CeTe}$ , there is, in the average, a slight decrease of the hybridization strengths below the Fermi level for both symmetries, namely  $\Gamma_7$  and  $\Gamma_8$ , but  $\Gamma_8$  is the one which shows the largest decrease. This last effect is to be attributed to the fact that  $\Gamma_8$  comes mainly from  $p$ - $4f$  mixing and, that the withdrawn charge is essentially of  $p$  character. This growing difference between both hybridization strengths is the reason for the experimentally observed larger values of the crystal field splittings, as compared to the splitting cor-

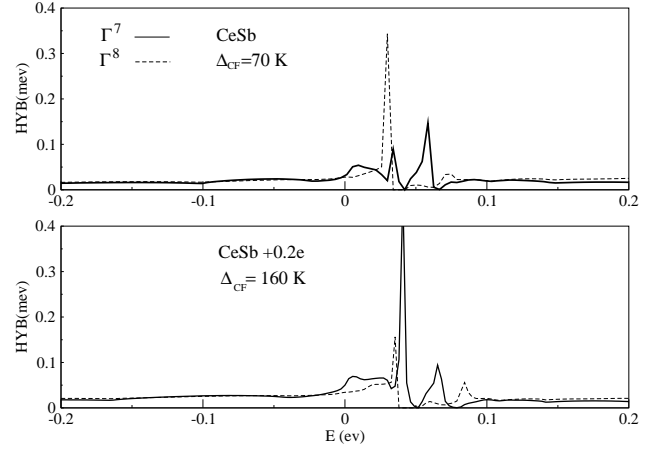


Figure 5:  $\Gamma_7$  and  $\Gamma_8$  hybridization functions around the Fermi level for:  $\text{CeSb}$  (upper panel) and  $\text{CeSb}+0.2$  (lower panel).

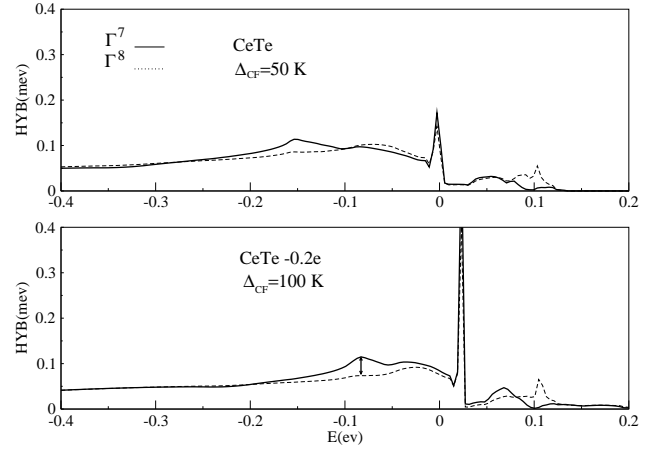


Figure 6:  $\Gamma_7$  and  $\Gamma_8$  hybridization functions around the Fermi level for:  $\text{CeTe}$  (upper panel) and  $\text{CeTe}-0.2$  (lower panel).

responding to  $\text{CeTe}$ . In Figure 6 it can be seen that  $\Gamma_7$  is larger than  $\Gamma_8$  below  $E_F$  for the system  $\text{CeTe} - 0.2e$  (lower panel). In this plot, we indicate the symmetry separation (between  $\Gamma_7$  and  $\Gamma_8$ ) with an arrow.

#### IV. DISCUSSION AND CONCLUSIONS

We apply in this work an *ab initio*-many body technique (LDA-NCA) to calculate the crystal-field splittings of the mononictides  $\text{CeX}$  and the monochalcogenides  $\text{CeY}$  series and their alloys. Within the *ab initio* frame, in which the  $4f$  states are treated as part of the valence band, we calculate the hybridization function  $\Gamma_{mm'}(\varepsilon)$ , which contains detailed information on the electronic structure of each material. This  $\Gamma_{mm'}(\varepsilon)$  function is used as input for the Anderson impurity model hamiltonian, which is solved within a multi orbital non-crossing approximation in the  $U \rightarrow \infty$  limit.

We show that the LDA-NCA technique gives the cor-

rect trends for the evolution of the crystal-field splittings of these systems, being the results in good agreement with the available experimental data [14] and with previous theoretical calculations [1]. We also obtain the correct symmetry for the ground state of the 4f multiplet, that is, the  $\Gamma_7$  one for all the compounds and alloys. In particular, we correlate the sudden decrease of the  $\Delta_{CF}$  when going from CeAs to CeSb (which are isoelectronic), to a big volume change.

The most important contribution to the values of the crystal-field splittings comes from energies around the Fermi level. We obtain that the hybridization strength around  $E_F$  is due mainly to the 5d-4f mixing. In those systems where the 4f states are more localized (CeBi, CeSb, CeTe) the intensity of the 5d-4f and of the p-4f hybridizations is smaller than in those where they are more delocalized. Due to this facts, magnitudes that depend on them, such as the crystal field splittings, are attenuated with respect to those compounds in which the 4f states more delocalized.

When comparing the results obtained for CeX with those for CeY, we obtain that the outcoming crystal-field splittings of the first series are slightly larger than those of the second one even if the CeY series has one more p electron. This is attributed to the fact that in the CeX

series the Fermi level falls in a maximum of the 5d-DOS while in the CeY one it does it in a valley. The effect of the extra p electron in CeY is to produce an enlargement of the  $\Gamma_8$  hybridization far below the Fermi level, and this does not influence the value of the splitting considerably.

Finally, we analyse the evolution of the splittings in the  $\text{CeX}_{1-x}\text{Y}_x$  alloys as a function of x. We consider one of the 'heavy' alloys, namely  $\text{CeSb}_{1-x}\text{Te}_x$ , and one of the 'light' ones,  $\text{CeAs}_{1-x}\text{Se}_x$ . Alloying gives rise to a non monotonic evolution of the  $\Delta_{CF}$ 's which according to our results, obtained within the virtual-crystal approximation, can be explained as an electronic effect by the only consideration of the added extra charge and to its effect on the hybridization functions.

## V. ACKNOWLEDGMENTS

This work was partially funded by UBACyT-X115, PICT-0310698 and PIP 2005-2006 Num. 6016. A. M. Llois and V. L. Vildosola belong to CONICET (Argentina).

- 
- [1] J. M. Wills and B. R. Cooper, Phys. Rev. B **36**, 3809 (1987).
  - [2] J. E. Han, M. Alouani, and D. L. Cox, Physical Review Letter **78**, 939 (1997).
  - [3] G. Kotliar and D. Vollhardt, Physics Today **57**, 53 (2004).
  - [4] B. R. Cooper, R. Siemmann, D. Yang, P. Thayamballi, and A. Banerjee, *Handbook of the Physics and Chemistry of the Actinides*, vol. 2 (edited by A. J. Freeman and G. H. Lander, North-Holland, Amsterdam, 1985).
  - [5] B. R. Cooper and O. Vogt, J. Phys. (Paris) Colloq **32**, C1 (1971).
  - [6] N. Kioussis, B. R. Cooper, and J. M. Wills, Phys. Rev. B **44**, 10003 (1991).
  - [7] P. Blaha, K. Schwarz, P. Sorantin, and B. Trickey, Comput. Phys. Commun. **59**, 399 (1990).
  - [8] O. Gunnarsson, O. K. Andersen, O. Jepsen, and J. Zaanen, Phys. Rev. B **39**, 1708 (1989).
  - [9] V. L. Vildosola, A. M. Llois, and M. Alouani, Phys. Rev. B **71**, 184420 (2005).
  - [10] P. Blaha, K. Schwarz, G. Madsen, D. Kvasnicka, and J. Luitz, *An augmented Plane Wave + Local Orbitals Program for Calculating Crystal Properties* (Karlheinz Schwarz, Techn. Universitat Wien, Austria, SBN 3-9501031-1-2., 1999).
  - [11] N. E. Bickers, Rev. Mod. Phys. **59**, 845 (1987).
  - [12] N. E. Bickers, D. L. Cox, and J. W. Wilkins, Phys. Rev. B **36**, 2036 (1987).
  - [13] M. R. Norman, D. D. Koelling, A. J. Freeman, H. J. F. Jansen, B. I. Min, T. Oguchi, and Ling Ye, Phys. Rev. Lett **53**, 1673 (1984).
  - [14] H. Heer, A. Furrer, W. Hälg, and O. Vogt, J. Phys. C: Solid State Phys. **12**, 5207 (1979).
  - [15] M. Nakayama, H. Aoki, A. Ochiai, T. Ito, H. Kumigashira, T. Takahashi, and H. Harima, Phys. Rev. B **69**, 155116 (2004).
  - [16] J. Rossat-Mignod, J. M. Effantin, P. Burlet, T. Chattopadhyay, L. P. Regnault, H. Bartholin, C. Vettier, O. Vogt, D. Ravot, and J. C. Achard, J. Magn. Magn. Mater. **52**, 111 (1985).
  - [17] N. J. Ramer and A. M. Rappe, Phys. Rev. B **62**, R743 (2000).
  - [18] I. I. Mazin, Appl. Phys. Lett. **77**, 3000 (2000).